Microstructural, Immunoreactivity and Biochemical Studies of the Cerebellum After Artequin Administration in Adult Wistar Rats

ABSTRACT

Aims: Artequin (ATQ) is a combination therapy antimalarial drug. Its effects on the microstructural, immunoreactivity and biochemical parameters were investigated in the cerebellum of adult Wistar rats.

Study design: Forty-two inbred adult male Wistar rats of average weight 200 g were divided into groups 1–6. Group 1 served as the control that received 5 ml kg^{-1} of water, while groups 2–6 received oral doses of 0.86/1.07 mg kg^{-1} (ATQ1), 1.71/2.14 mg kg^{-1} (ATQ2), 3.42/4.28 mg kg^{-1} (ATQ3), 6.84/8.56 mg kg^{-1} (ATQ4) and 13.68/17.12 mg kg^{-1} (ATQ5) body weight of artequin for three days

Place and Duration of Study: This research took place at the Department of Zoology, Faculty of Biological Sciences, Akwa Ibom State University, Nigeria and Department of Anatomy, Faculty of Basic Medical Sciences, University of Uyo, Akwa Ibom State, Nigeria, between June 2024 and July 2024.

Methodology: The animals were sacrificed after they were deeply anesthetized with ketamine–hydrochloride. Biochemical assays for oxidative stress were carried out for superoxide dismutase, malondialdehyde and catalase. The brains were perfused fixed in 10 % buffered formalin. They were processed using haematoxylin and eosin, Bielschowsky silver impregnation and immunohistochemical labelling for glial fibrillary acidic proteins.

Results: There was a high significant difference (P = .05) in serum concentration of malondialdehyde in ATQ5 when compared to the control and the other treatment groups; there was no significant difference in superoxide dismutase and catalase between the artequin groups and the control group. The cerebellum of the ATQ groups showed histopathological features including cell atrophy, pyknosis, karyorrhexis, hypertrophy and decreased (P = .05) cellular densities, with increased expressions of glial fibrillary acidic proteins when compared with the control group.

Conclusion: Artequin administration induced a dose-dependent adverse effects on the microstructure and GFAP immunolabelling of the cerebellum. This may suggest neuronal and glial degeneration, thus resulting in altered cerebellar functions

Keywords: *Combination therapy, artequin, cerebellum, histopathology, glial fibrillary acidic proteins (GFAP)*

1. INTRODUCTION

According to Udofia *et al.,* (2022), malaria is a parasitic disease transmitted to humans by infectious female mosquitoes of the genus Anopheles. It is caused by protozoan parasites of the genus Plasmodium with five species *Plasmodium falciparum, P. ovale, P. vivax, P. malariae* and *P. knowlesi* affecting humans (Udofia *et al.,* 2022). According to the World Health Organization, malaria caused by *P. falciparum* is a severe form of the infection which had resulted in about 228 million cases and 608,000 deaths at as the year 2022, with 76% of the reported death recorded in children under 5 years (WHO, 2024). The most successful attempts at treatment includes the simultaneous use of two or more artemisinin-based drugs with independent modes of action and different biochemical targets in the *Plasmodium* parasite. This use of artemisinin-based combination therapy (ACT) was due to the reported cases of resistance from monotherapies in the treatment of *P. falciparum* malaria infection. ACT offers several advantages, including reduced risk of treatment failure and resistance, and enhanced convenience (Handboonkunupakarn *et al.,* (2019); WHO, (2015).

Artequin is among the ACTs recommended by the WHO in the treatment of all forms *P. falciparum* malaria infections. It is a combination of two highly potent drugs, namely, artesunate and mefloquine (Sodiomon *et al.,* (2016); Udoh *et al.,* (2014); Udoh *et al.,* (2020). Atesunate is a water soluble, semi synthetic, sesquiterpene lactone derived from the Chinese medicinal herb *Qinghua* (Kouakou, *et al.,* (2019); Mohammadi *et al.,* (2020) It effects on the parasite is quick in reducing the parasite load, but its action has a short half – life (Udoh *et al.,* (2014); Mohammadi *et al.,* (2020). Mefloquine on the other hand, is a 4-quinoline methanol blood schizonticide

with a long-acting half-life, which takes over the protection against re-infection (Kouakou, *et -al.,* (2019); Roche, (2011). These properties complement and protect each other against the development of resistance (Sodiomon, *et al.,*2016).

However, it has been reported that mefloquine and artequin administration adversely affects some areas of the brain such as the hippocampus, resulting in hypertrophy, pyknosis, reduced pyramidal cell density with increased expressions of glial fibrillary acidic protein (GFAP) (Ekanem *et al.,* (2009); Udoh *et al.,* (2014); Udoh *et al.,* 2020). A report illustrated that the hippocampus is functionally connected to the cerebellum in a bidirectional manner, such that the hippocampus can influence cerebellar activity and vice versa in health and in disease (Yu and Magnuson (2015).

The cerebellum is the largest portion of the hindbrain. Its principal function is to regulate and maintain balance, and to coordinate timing and precision of body movement (Harold and Vishy (2010); Wolf *et al.,* (2009) it also plays an important role in cognition (Wolf *et al., (*2009). The cerebellum has multiple connections with other parts of the brain such as the brain stem, thalamus, vestibular nuclei and the hippocampus (Harold and Vishy (2010); Yu and Magnuson, (2015). This enables it to constantly monitor sensory inputs from effector organs and then refine and coordinate their responses (Harold and Vishy (2010).

Since the cerebellum and the hippocampus are functionally related in a bidirectional manner (Yu and Magnuson, 2015), and given the fact that even at lower concentrations, mefloquine administrations have been reported to show histopathological features in the hippocampus (Udoh *et al.*(2014); Ekanem *et al.,* (2009); Udoh *et al.,* (2020), as well as adverse effects such as inhibition of electrical coupling of neurons, resulting in the destruction of spiral ganglion neurons and auditory nerve fibers (Allison *et al.,*(2001); Da–lian,*et al.,* (2009); Dowl *et al.,* (2006); Steffensen *et al.,*(2011), the presence of mefloquine in artequin may affect the cerebellum, necessitating this study on the effects of this drug on the cerebellum when not properly used. Thus, this study aimed to investigate the effects of the combination therapy, artequin, on the cerebellum microstructure, immunoreactivity, as well as on the biochemical parameters of adult Wistar rats.

2. MATERIALS AND METHODS

"Forty-two inbred adults male Wistar rats of average weight 200 g, were obtained and housed in the Animal House of the Faculty of Basic Medical Sciences, University of Uyo, Nigeria. The animals were housed in 14 standard home cages (40 cm × 35 cm) with wire gauze roof and wood shavings beddings. This study took place in the month of June whereby the room temperature was between 27^{o}C – 30^{o}C, and the animals were exposed to 12:12 hours light/dark cycles and fed with normal commercial pelletized growers mash (Vital Feed Grand Cereal Ltd, Jos, Nigeria) and clean water *ad-libitum*. The animals were allowed to acclimatize for fourteen days before commencement of the experiment. The animals were handled according to international guidelines as laid down by the National Institute of Health (NIH) of the United States of America for the regulation of laboratory animals" (National Institute of Health, 2011).

Artequin (J0004912, Acino Pharmaceutical limited, Switzerland) was obtained from the University of Uyo Pharmacy, Uyo, Nigeria. The Artequin was dissolved in 100 mL of distilled water. The therapeutic dosages for the rats were determined against the therapeutic doses for humans, which is 600/750 mg kg^{-1} of artequin.

2.1 Animal Grouping and Administration of Artequin

The Wistar rats were divided into six groups of seven animals each, modified from Udoh *et al.,* (2014). Group 1 was the control group. Groups 2 - 6 served as the treatment groups. Each co-blister tablet of artequin (ATQ, artesunate, 600 / Mefloquine, 750 mgkg^{-1}) dissolved in 100 mL of distilled water was administered to the animals orally with the aid of orogastric tubes for three days according to their body weights (Table 1).

Table 1. Dosages of drugs administered to the rats for three days

Groups (n-6)	Drugs	Dosages /day
1 (Control)	Water	5 mL kg^{-1}
ATQ $_1$	ATQ (LD eqv.)	0.86/1.07 $mgkg^{-1}$
ATQ $_2$	ATQ (LD eqv.)	1.71/2.14 $mgkg^{-1}$
ATQ $_3$	ATQ (TD eqv.)	3.42/4.28 $mgkg^{-1}$
ATQ $_4$	ATQ (HD eqv.)	6.84/8.56 $mgkg^{-1}$
ATQ $_5$	ATQ (HD eqv.)	13.68/17.12 mg kg^{-1}

**ATQ = Artequin LD eqv = low dose equivalent = TD eqv.: therapeutic dose equivalent = HD eqv = high dose equivalent*

2.2 Tissue Processing

The animals were sacrificed after they were deeply anesthetized with 60 mg kg^{-1} ketamine–hydrochloride (#50155, Rotex Medica, Trittau, Germany). Blood samples for biochemical assays were immediately collected intra-cardially with the aid of 2 ml syringe for each animal. The blood samples for superoxide dismutase and malonaldehyde assays were stored in ethylene diamine tetra acetic acid (EDTA) bottles marked and labelled for each animal. Samples for catalase demonstration were stored in 10 ml plastic test tubes in ice, marked and labelled for each animal. Intra - cardial perfusion with phosphate-buffered saline (PBS, 2M, pH 6.4), were carried out by means of a cannula and then perfused-fixed with 10% buffered formalin. On complete perfusion, the skull was opened and the brain of the animal removed and post fixed in 10% buffered formalin for 48 h. The whole cerebellum was further routinely processed for histological studies using haematoxylin and eosin (Ellis, 2019), and Bielschowsky silver impregnation (Neurotech, 2012) methods respectively. Representative sections were also used for glial fibrillary acidic protein immunolabelling (IHCWORLD 2019). Sections were viewed under the light microscope and photomicrographs were obtained using the microscope camera linked to a computer.

2.3 Determination of Cellular Density

Cellular population of the three cortical layers of the neocerebellum was carried out by means of Image™ software linked to a computer. This approach involved manual cell counting and marking of the cells with the help of a plugin, modified after (Bindokas, *et al.,* 2020). This technique allows cell count by clicking on the image. Each click marks the cell with a coloured square and then adds the cell to a tally sheet. The cellular population for each neocerebellar cortical layer was marked, tallied separately with a different colour square. After each counting session, the result for the total of all the cells in the three cortical layers plus the grand total of all the clicks was displayed at the bottom of the result window. This result log was copied and pasted in an excel spreadsheet for statistical analysis. The same procedure was repeated for the photomicrographs in all the groups as described by (Bindokas, *et al.,* 2020).

2.4 Biochemical Test

Biochemical assays for oxidative stress were carried out for superoxide dismutase, malondialdehyde and catalase. Assay for superoxide dismutase and malondialdehyde were carried out using EDTA bottles as an

anticoagulant. Blood samples were centrifuged for 15 minutes at 2 – 8^{o}C at 120 rotations per minute within 30 minutes of collection. The supernatants were collected and the assay carried out immediately. All reagents were brought to room temperature before use. The samples were centrifuged again at 120 rotations per minute after thawing before the assay. All the reagents were mixed thoroughly by gentle swirling before pipetting. Foaming was avoided and all samples and standards were assayed in duplicates as highlighted in ELISA Kit user manual (Elabscience $^{(R).}$ (2016a and b) and modified after the method described by Giera *et al.,* (2012). Assay for catalase was conducted using 0.5 ml hydrogen tetraoxosulphate (H_2SO_4) added to 0.5 ml of 0.24 substrate solution properly mixed together. The mixture was titrated with standard permanganate till a faint pink colour was obtained. The titre was read off the pipette. Afterwards 0.5 ml of 0.24 substrate solution and 0.1 ml hemolysate were added into a universal container. These were allowed to react for 5 minutes before the reaction was stopped with 0.5 ml H_2SO_4 mixed well. The solution was then titrated with 0.005 molar potassium permanganate ($KMNO_4$) till a permanent light pink colour was obtained. Titre values were then read off the pipette, modified after Mahmoud, (2016) and Thulfegar *et al.,* (2020).

2.5 Statistical Analysis

One-way analysis of variance was used to analyse all the data, followed by a *post hoc* Tukey's test. All analysis was done using GraphPad Prism for Windows (version 5.01, San Diego California, USA). Data at probability level P = .05 was regarded as significant and are presented as Mean ± Standard error of mean.

3. RESULTS:

3.1 Biochemical Assay of Some Oxidative Markers: There was a significantly higher (P = .05) malondialdehyde level in the ATQ5 group compared with the control and other test groups. However, there was no significant difference in serum concentration of superoxide dismutase and catalase between the artequin groups and the control group (Figure 1).

3.2 Histomorphological/Histomorphometry Observations: Haematoxylin and eosin (H and E): Sections of the cerebellum of the control rat showed well-arranged neuronal cells in the molecular cell layer with spherical shaped Purkinje cell bodies in the Purkinje layer and densely packed cells in the granular layer (Plate 1a). ATQ1 animals, showed hypertrophied Purkinje cell neuron, while the cells in the other layers appear unaffected (Plate 1b). Sections of the cerebellum of ATQ2 animals showed marked hypertrophied Purkinje cell neurons with pyknotic nuclei in the Purkinje cell layer, the granular cells appear atrophied compared with the control group;

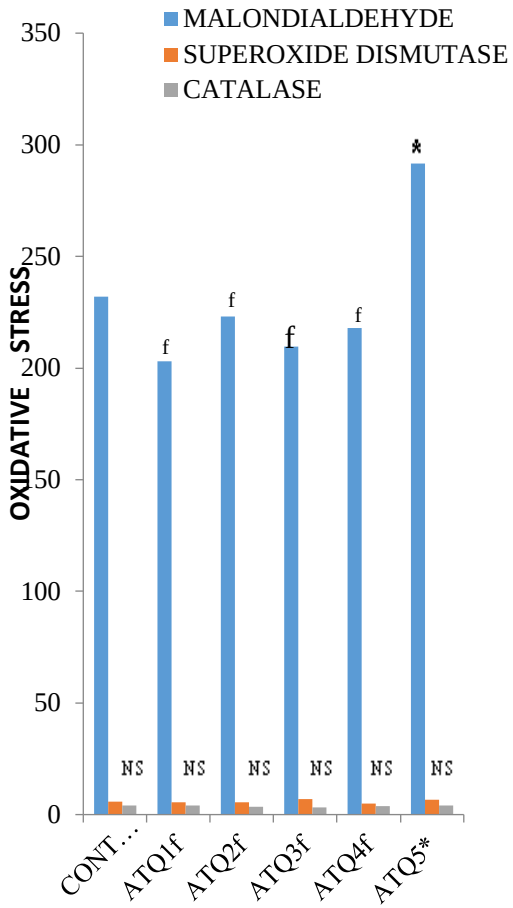

Figure 1. Biochemical assay of some oxidative markers, Data are presented as mean ± standard error of mean

** Significantly different from the control group at p<0.05*

F Significantly different from group AQ5 at p<0.05

NS Not significantly different from the control group at p<0.05

ATQ= Artequin

the cells in the molecular layer appear unaffected (Plate 1c). The sections of the cerebellum of ATQ3, ATQ4 and ATQ5 animals showed hypertrophied Purkinje cells with pyknotic nuclei in the Purkinje cell layer and atrophied granular cells compared with the control group. The molecular layer appears unaffected (Plates 1d, e and f).

Cellular Density: The cellular density of sections of the cerebellum in the entire test groups was significantly lower (P =.05) compared with the control group. All the other test groups were significantly lower (P = .05) compared with ATQ2 (Figure 2)

Silver Impregnation: Sections of the cerebellar cortex of the control animals showed spherical shaped Purkinje cell bodies in the Purkinje cell layer with densely packed cells in the granular layer cells (Plate 2a). Sections of the cerebellar cortex of the ATQ1 and ATQ2 animals showed degenerating Purkinje cell neurons with silver grains, while the molecular and granular showed cell layers appear unaffected (Plates 2b and c). The sections of the cerebellar cortex of ATQ3 animals showed hypertrophied Purkinje and granular cells with increased arborization

of dendritic processes in the molecular layer (Plate 2d). Sections of the cerebellum of ATQ4 and ATQ5 animals showed degenerating Purkinje, molecular and granular cells with argyrophilic nuclei (Plates 2e and f)

Immunolabelling Observations: The sections of the cerebellum of the control group and ATQ1 animals showed little expression of glial fibrillary acidic protein throughout the cortical layers (Plates 3a and b). Sections of the cerebellum of ATQ2 and ATQ3 animals showed increased expressions of glial fibrillary acidic protein, stained reactive astrocytes and astrocytes' processes throughout the cortical layers compared to the control (Plates 3c and d). The sections of the cerebellum of ATQ4 and ATQ5 animals showed marked expressions of glial fibrillary acidic protein with thin films of GFAP expressing astrocytic processes compared to the control (Plates 3e and f).

4. Discussions

In the present study, the cerebellar microstructure, immunolabelling and biochemical parameters were investigated upon artequin administration. In - vivo control of the accumulation of reactive oxygen species as a result of lipid peroxidation is controlled by non-enzymatic antioxidant systems and defense-related enzymes such as superoxide dismutase, catalase and glutathione peroxidase (Giera, *et* al., (2012). Malondialdehyde appears to be the most mutagenic product of lipid peroxidation (Mariona *et al.,* (2020). Compared with other reactive oxygen species, malondialdehyde has a relatively longer half – life and a non – charge structure, which makes it a potentially more destructive compound, since it can affect all structures and distant macromolecules within its vicinity (Pamplona, 2008). Lipid peroxidation is a well-established mechanism of cellular injury in both plants and animals. It is used as an indicator of oxidative stress in cells and tissues (Giera *et al.,*2012). The measurement of malondialdehyde, which is the most abundant of lipid peroxidation products, such as in this present study, is a convenient and sensitive method for quantitative estimation of lipid peroxide concentration in many types of samples including drugs, food products and biological tissues from human and animal (Mariona *et al*.,2020). The presence of malondialdehyde has been shown to relate to the pathophysiology of various diseases and the assay of serum or plasma malondialdehyde make it a valuable tool for clinical management (Li *et al.,* 2010).

In this present study, there was a significantly higher (P = .05) malondialdehyde level in the ATQ5 group compared with the control and other test groups. However, catalase and superoxide dismutase showed no significant difference in serum concentration between the artequin groups and the control group. This result indicates that lipid peroxidation process was not properly regulated and the defense mechanism was not balanced by the antioxidant enzymes, superoxide dismutase and catalase upon the administration of artequin. The result in the present study relates to earlier reports by Inal *et al.,* (2001) who reported that the activity of antioxidant enzymes in response to the accumulation of reactive oxygen species is equivocal, with both increased and decreased activities (Inal *et al.,*2001). The result in the present study agrees with a previous report by Li *et al,* (2010), who reported that high levels of malondialdehyde suppresses cerebral function by breaking homeostasis between excitation and inhibition. This may have been the case in the present study on the cerebellum Hence, this failed defense mechanism apparent in the present study by a lack of significance difference in the serum concentrations of superoxide dismutase and catalase must have resulted in an increased levels of reactive oxygen species and oxidative stress. This is shown by the increase in malondialdehyde level in the treatment groups with higher dosage of artequin (ATQ5). According to Mariona, *et al.,* (*2020)*, low concentrations of malondialdehyde leads to longevity of the cells, tissues and life of animal species. This indicates that a high malondialdehyde concentration is capable of injuring membrane lipids, proteins and nucleic acids as seen in the micromorphological presentations of the artequin groups in the present study.

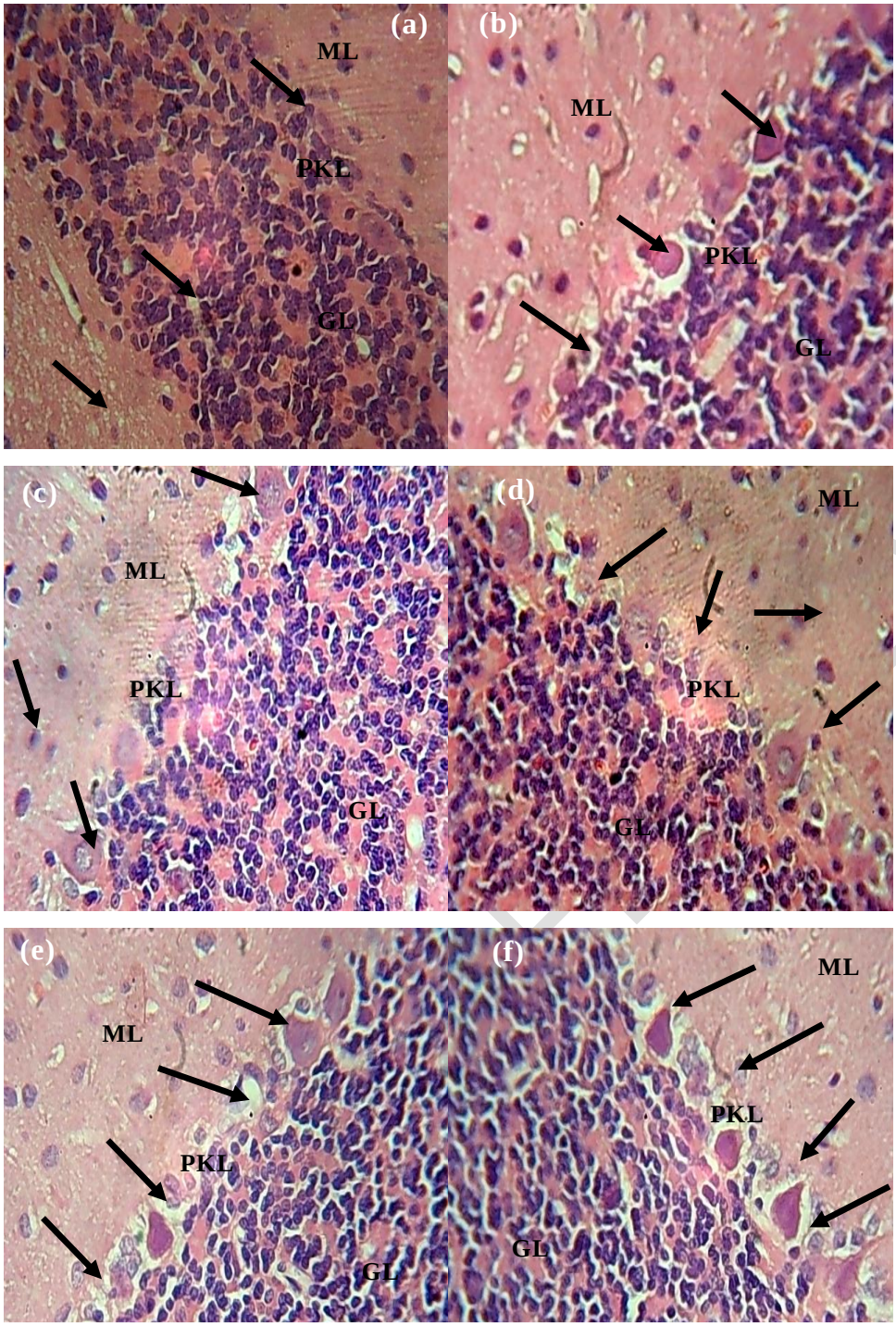

Plate 1. The sections of the cerebellum of the control and test group: H & E x400. (a)Control, (b)ATQ1, (c)ATQ2, (d)ATQ3, (e)ATQ4, (f)ATQ5

Sections of the cerebellum of control group showing normal histological appearance of neurons and glia in the Purkinje cell layer (PKL), granular layer (GL) and the molecular layer (ML) with hypertrophied Purkinje cell neuron (short arrow) in the ATQ1 group. Sections of the cerebellum of ATQ2 and ATQ3 shows markedly hypertrophied molecular and Purkinje neuron with pyknotic nuclei (arrows). The granular cells appear atrophied, while ATQ4 and ATQ5 cerebellar sections shows markedly hypertrophied molecular and Purkinje cell neuron with pyknotic nuclei (arrows). The granular cells appear atrophied.

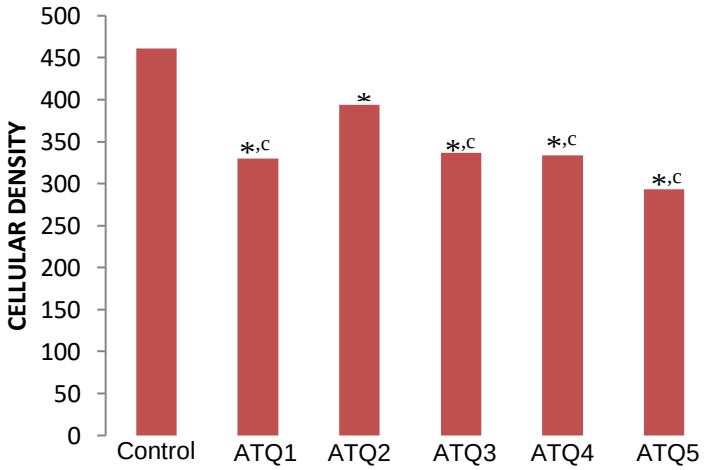

Figure 2. Cerebellar cellular density in the control and test groups

**Significantly different from the control group at P = .05*

c Significantly different from the ATQ2 at P =.05

Therefore, the increased dosages of artequin administered in this present study did induce oxidative stress which was more apparent in the ATQ5 group

Histological findings of the cerebellum of the animals that received artequin in all the treatment groups showed alterations including cell atrophy, hypertrophy, karyorrhexis and pyknosis in the artequin groups compared to the control group. These histopathological features are the same seen in lead poisoning previously reported by Okon *et al.,* (2022). The cerebellum is involved in motor control and cognitive functions with a well-defined fine movement-related coordination (Wolf, *et al.,*2009). This is made possible by its primary cells called the Purkinje. The Purkinje cells have large triangular shaped soma with distinctive activity pattern which makes them capable of receiving more synaptic inputs than any other type of cell in the brain (Shi *et al*., 2008). However, damages to the cerebellum upon the administration of the antimalarial artequin, as seen in this present study can exacerbate impaired cerebellar activity resulting in altered inter-relational functions. This is possible because, the histopathological presentations in the artequin groups are all features of type-two neuron deaths as described by Pagnussat, *et al.,* (2007). These degenerative features which was previously described by Jonah *et al., (*2022) especially in the Purkinje neurons in the artequin groups as seen in the present study may hinder the participatory role of the Purkinje cells as the primary excitation unit in cerebellar function.

Changes in brain cellular densities have been reported by Ekong *et al.,* (2014). In this present study, the cellular density of the cerebellum of the entire artequin groups were lower compared with the control group. This is because the administration of artequin may have caused a decrease in the expression of glutamic acid decarboxylase 67, which is a major gamma amino butyric acid synthesizing enzyme which functions to enhance cell growth in cerebellar Purkinje neurons (Ravi *et al.,*2014). This suggests that artequin administration may have damaged these GABAergic neurons leading to decrease in the cerebellar density via the downregulation of glutamic acid decarboxylase 67 in the Purkinje cell nuclei. The data in this present study agrees with the report on the decrease in cerebellar cortical density in adult Wistar rats upon the administration of artesunate, as well as lower Purkinje cell nuclei in psychosis and essential tremor (Ekrem, *et al.,*2010; Ravi *et al.,*2014).

Bielschowsky silver impregnation (Neurotech, 2012) which was adopted in this present study is used to visualize neurites as well as the cell bodies of neurons undergoing neurodegeneration. The principle of this technique relies on the localized absorption of anions which form insoluble complex with added silver ion. The anion impregnates

the tissue and the silver ion is used to aid in visualizing the reaction by forming insoluble complexes. The silver ion in this complex is then reduced to metallic silver grains by an exogenously applied reduced agent. In this present study, the cortical sections of the cerebellum of the animals in all the artequin groups showed cytoarchitectural alterations with strong affinity of the cells to silver ions in the degenerating Purkinje cell layer and axonal terminals. The initial step during silver impregnation is followed by a reduction step during which the silver seed are enlarge with a reducing agent in an alkaline environment that reduces the silver ions to metallic grains which are visible in the cell bodies, axons and dendrites undergoing neurodegeneration as seen in the ATQ groups. In this present study, the Purkinje cells showed several distinct features including disorganization and proliferation of processes of basket cells in the molecular layer, and some surrounding degenerating Purkinje somas (Plate 4d and e). According to Jonah *et al.,* (2022) and Ferrer *et al.,* (2008) the occasional loss of Purkinje cells usually results in the presence of degenerative axon terminals surrounding an empty space in the cerebellum. This may have been the case as seen in all the artequin groups in this present study. The principle of silver impregnation technique is based on the findings that certain component of neurons undergoing degeneration become particularly argyrophilic (Mitra *et al.,*2009). This argyrophilic metallic grains are visible under the light microscope upon reduction. The onset of argylophilic grain can result in cognitive decline and behavioural abnormalities (Ferrer *et al.,*2008; Neurotech, 2012), as seen in this present study.

Immunolabelling of the cerebellar cortical layers of rats treated with artequin showed various degrees of astrogliosis, characterised by increased GFAP expressing astrocytes and astrocytic. processes.

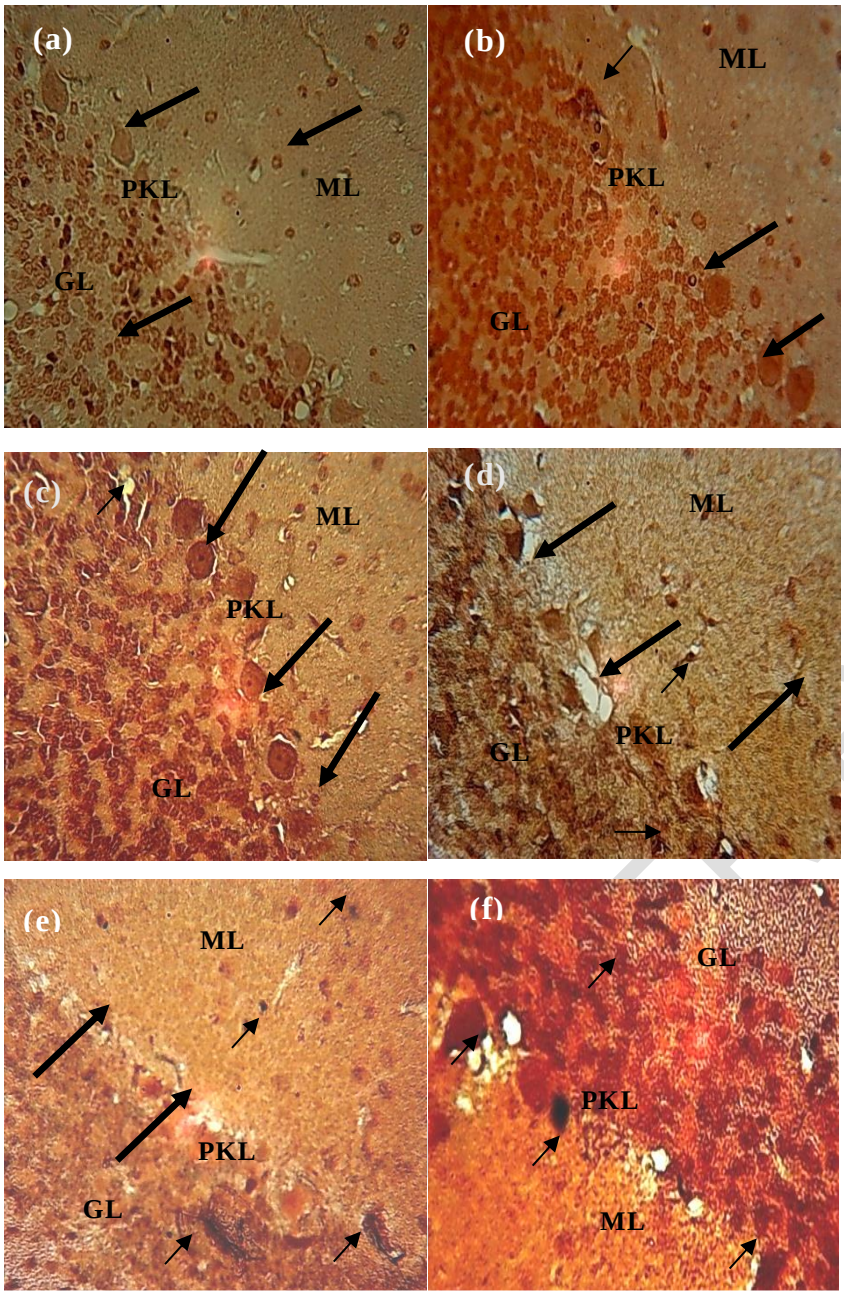

Plate 2. Sections of the cerebellum of control and test group. Silver impregnation x400. (a)Control, (b)ATQ1, (c)ATQ2, (d)ATQ3, (e)ATQ4, (f)ATQ5

Sections of the cerebellum of control rat showing normal appearance of neurons and glia in the three cortical areas (arrows). ATQ1 -ATQ2 shows hypertrophied (arrow) and argyrophilic Purkinje cell nuclei (short arrow) in the Purkinje cell layer (PKL). ATQ3 Shows degenerating neurons and axonal terminals (arrows) throughout the three cortical layers with visible argyrophilic nuclei layers (short arrows). ATQ4 shows degenerating Purkinje cells nuclei in the Purkinje cell layer (arrows) with argyrophilic grains throughout the tree cortical layers (short arrows). The granular cells appeared unaffected. ATQ5 showing degenerating Purkinje, granular and molecular layer cells with argyrophilic nuclei (short arrows). ×400

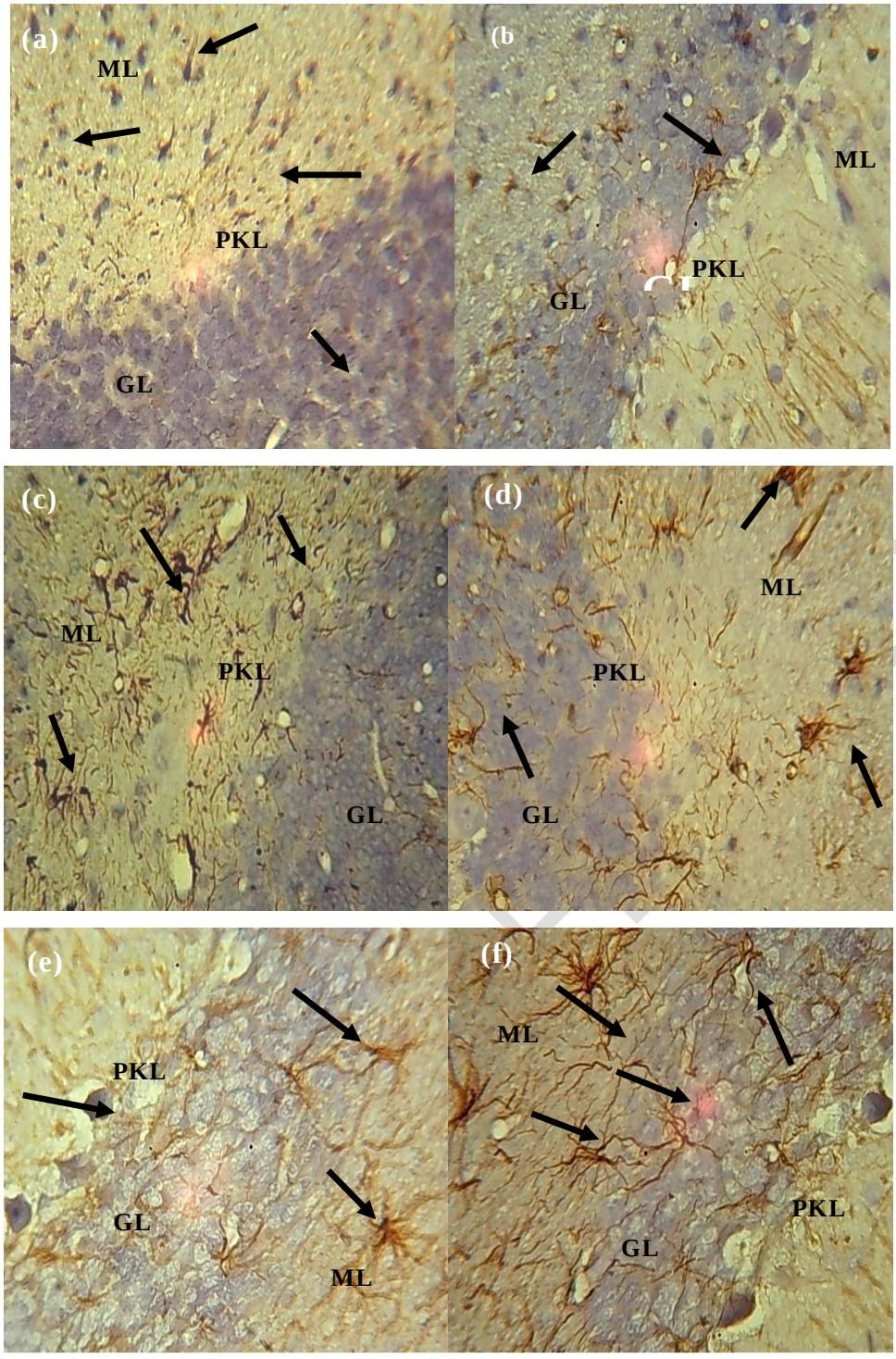

Plate 3. The sections of the cerebellum of control and test groups: GFAP x400. (a)Control, (b)ATQ1, (c)ATQ2, (d)ATQ3,(e)ATQ4,(f)ATQ5 x400

The control and the ATQ1 groups showing scanty/little expression of glial fibrillary acidic protein (GFAP) (arrow)throughout the cortical layers (arrows). ATQ2 -ATQ3 groups shows visible expressions of GFAP stained reactive astrocytes and processes in the cortical layers (arrows). There is also wide expression of glial fibrillary acidic protein (GFAP) (arrows) with thin films of vacuolations marked with GFAP stained astrocyte processes around degenerating cells in the ATQ4 and ATQ5 cerebellar sections.

Insults to the brain triggers a complex GFAP astroglial response called 'reactive astrocyte' which is manifested by astrocyte hypertrophy and proliferation (Pekny and Nilsson, 2005). Udoh *et al.,* (2020) had reported that reactive GFAP astrogliosis is a defensive brain reaction aimed at isolating damaged areas from the rest of the central nervous system tissues. It also reconstructs the blood–brain barrier and facilitates the remodelling of brain circuits in areas surrounding the lesioned region (Roche, 2011). In animals with genetically deleted GFAP, astroglial scar is formed slowly and the healing of brain traumas is generally prolonged (Verkhratsky, and Arthur, 2007). In this present study, immunolabelling of the cerebellar cortical layers of ATQ2, ATQ3, ATQ4 and ATQ5 animals, revealed increased GFAP expressing reactive astrogliosis. However, animals treated with lower dosages of artequin such as the ATQ1 group showed non-reactive GFAP expressions. Astrogliosis ultimately ends up in complete substitution of previously existing tissues architecture with permanent glial scar prolonged (Verkhratsky, and Arthur, 2007). This leads to the inhibition of axonal regeneration and the prevention of nerve processes from entering the damaged zone by the production of chondroitin and keratin (Tani *et al.,*2005; Reza *et al.,* 2014). These may be the case in the artequin groups in this present study as the increase in reactive astrocyte is to possibly ameliorate the effects of the insult caused by artequin through the release of mucopolysacharide which will eventually cement the areas of damage in the artequin groups. The result of this present study agrees with similar work reported on mefloquine and artequin in the hippocampus by EKanem *et al.,* (2009), Udoh *et al.,* (2014) and Udoh *et al.,* (2020). The presence of these GFAP expressions in some of the artequin groups points to the fact that artequin administration resulted in insult to the cerebellum that may result in neuronal and glial pathology in this present study, which may lead to hindered physiological activity of this brain area.

5. Conclusion

This study showed that oral administration of artequin resulted in high level of serum malondialdehyde, indicating oxidative stress. The cerebellar microstructure showed histopathological features such as hypertrophy, pyknosis, Karyorrhexis and loss of cellular population which are all indications of insult or injury. The cerebellar cortical layers also showed GFAP astrogliosis, indicating trauma. The effects were in a dose dependent manner

ETHICAL APPROVAL:

The Faculty of Basic Medical Sciences Research and Ethical Committee (FBMSREC) (Ethical Number: UU_FBMSREC_2023_005) having undertaken a thorough review of your application and the revisions has approved your research to be carried out as described in the proposal

Disclaimer (Artificial intelligence)

Authors hereby declares that NO generative AI technologies such as Large Language Models (ChatGPT, COPILOT, etc.) and text-to-image generators have been used during the writing or editing of this manuscript.

REFERENCES

1. Udofia, L. E., Udoh, N. B., Edohoabasi B. G., & Owowo E. E. (2022). Antimalarial Activity of *Bambusa vulgaris* on *Plasmodium berghei berghei* in mice. Nigerian Journal of Parasitology ISSN 1117 4145 Volume 43[2] September,2022. https://dx.doi.org/10.4314/njpar.v43iXXX
2. World Health Organization. (2024). World Malaria Report. December 2024, WHO, Geneva, Switzerland.
3. Handboonkunupakarn, B., Vander-Plurjin, & Hogland R.W. (2019). Sequential Open – Label Study of the Safety, Tolerability and Pharmacokinetic Interaction Between Dihydroartemisinin – Piperaquin and Mefloquine in Healthy Thai Adult. Anti microb Agent Chemotherapy. 2019; 63
4. World Health Organization (2015). Guideline for the Treatment of Malaria- 3rd Edition,Geneva, Switzerland
5. Nsikan-Abasi B. Udoh, Theresa B. Ekanem, Moses B. Ekong, Aniekan I. Peter & Amabe O. Akpantah (2014) Hippocampal Glial Degenerative Potentials of Mefloquine and Artequin in Adult Wistar Rats. International Journal of Brain Science. Hindawi Publishing Corporation. International Journal of Brain Science Volume 2014, Article ID 104785, 5 pages http://dx.doi.org/10.1155/2014/104785
6. Sodiomon, B. S., Bernhards, O., John, P. A., Ali M., Zakayo M., & Alphonse., *et al.,* (2016). Comparison of Artesunate – Mefloquine and Artemether – Lumefantrine Fixed – Dose Combination for Treatment of Uncomplicated *P.falciparum* Malaria in Children Younger than 5 years in Sub – Saharan Africa;A Randamised Multicentre phase 4 Trial. Lancet; Infectious Diseases. Vol 16; 10, p1123 -1133
7. Nsikan-Abasi B. Udoh**,** Theresa B. Ekanem & Moses B. Ekong (2020). Behavioural and Microstructural Evaluation of the Hippocampus of Adult Wistar Rats Following Artequin Administration Current Research inNeuroscience 10 (1): 1-10,2020 10.3923/crn.2020.1.10, https://scialert.net/abstract/?doi=crn.2020.1.10 DOI: 10.3923/crn.2020.1.10
8. Kouakou, Yobouet Ines., Michel Tod., Gilles Leboucher., Adeline Lavoigut., Guillaume Bannot., & Anne – Lise Bienvenu., *et al.,* (2019). Systematic Review of Artesunate Pharmacokinetics: Implication for Treatment of Resistant Malaria. *International Journal of Inffectious Diseases.,* 89 (2019) 30 – 44
9. Mohammadi, S., Jafari, B., Asgharian, P., Martorell, M., & Sharifi – Rad (2020). Medicinal Plant Used in the Treatment of Malaria: a key Emphasis to Artemisia *Cinchona, Crytolepsis* and *Tabebuia genera. Phytotheraprutic Research* 34 (7):1556 – 1569.
10. Kouakou, Yobouet Ines., Michel Tod., Gilles Leboucher., Adeline Lavoigut., Guillaume Bannot., Anne – Lise Bienvenu., Stephane Picot. (2019). Systematic Review of Artesunate Pharmacokinetics: Implication for Treatment of Resistant Malaria. *International Journal of Inffectious Diseases.,* 89 (2019) 30 – 44
11. Roche: Lariam® (2011). Mefloquine hydrochloroquine. Medication guide. *Hoffman-La Roche*. 151(10):1013-1024.
12. Ekanem, T. B., Salami, E., Ekong, M. B., Eluwa, M., A. & Akpantah, A. O. (2009). Combination Therapy Anti -Malaria Drugs, Mefloquine and Artequin Induce Reactive Astrocyte Formation in the Hippocampus of Rats. *The International Journal of Health*, 9 (20): 46-51.
13. Yu, W. & Magnuson K, E. (2015). Cognitive collaborations: bidirectional functional connectivity between the cerebellum and the hippocampus. *Neuroscience*, 9(5): 177-187.
14. Harold. E., and Vishy M. (2010) Clinical Anatomy: Applied Anatomy for Students and Junior Doctors, 12th Edition, pp362 -363
15. Wolf, U., Rapoport, M. J. and Schweizer, T. A. (2009). Evaluating the Affective Component of the Cerebellar Cognitive Affective Syndrome. Neuropsychiatry and Clinical Neuroscience, 21 (3): 245–453.
16. Allison, D. W., Wilcox, R. S. & Ellefsen, K. L. (2001). Mefloquine effects on ventral tegmental area dopamine and GABA neuron inhibition: a physiologic role for connexin-36 gap junctions. *Synapse*, 65(2): 804 - 813.

17. Da–lian, D., Qi, W., Yu, D., Jiang, H. & Richard, S. (2009). Ototoxic Effects of Mefloquine in Cochlear Organotypic Cultures. *Journal of Otology*, 4 (2); 76–85.
18. Dowl, G., Bauman, R., Caridhal, D., Cabezas, M., Gomez-Lobo, R., Park, M., Smith, K. & Cannard, K. (2006). Mefloquine Induces Dose Dependent Neurological Effects in Rat Model. *Journal of American Society for Microbiology, Anti-microbial Agents and Chemotherapy*, 50 (3):1045- 1053.
19. Steffensen, S. C., Bradley, K. D. & Hansen, D. M. (2011). The role of connexin-36 gap junctions in alcohol intoxication and consumption. *Synapse,* 65(17): 695–707
20. National Institute of Health, (2011). Guide for the Care and Use of Laboratory Animals, 8th ed., Washington: National Academies Press, pp. 1 – 2.
21. Ellis,R., (2019). Hematoxylin and Eosin (Hand E) Staining Protocol, IMS's Division of Pathology. The Queen Elizabeth Hospital, Woodville Road, Woodville, South Australia, 5011, http//www.ihcworld.com/protocol/special_stain/h and e_ellis.htm.
22. Neurotech (2012). Neurosilver™ Kit II:A Rapid Silver Staining Kit for the Microscopic Detection of Neuronal Damage. FD NeuroTechnologies Consulting and Services, Inc., Columbia, pp:45.
23. IHCWORLD (2019). GFAP Antiboby Staining Protocol forImmunochemistry. http://www.ihcworld.com/protocol/antibody_protocol/gfap_novocastra.htm
24. Bindokas Vytas., Christian Labno., Shirley Bond & Benjamin Glick (2020). Two ways to Count Cells with ImageJ™ software.*Integrated Light Microscopy Core*, University of Chicago, Page 1 – 5
25. Elabscience (R). (2016a). *Malondialdehyde ELISA Kit User Manual*, Elabscience Biotechnology Limited, Wuhan: pp1- 13.
26. Elabscience (R). (2016b). *Superoxide Dismutase 3 Extracellular ELISA Kit User.* Elabscience Biotechnology Limited, Wuhan, pp2- 13.
27. Giera, M., Lingeman, H., & Niessen W. M. (2012). Recent advancements in the lc- and gc-based analysis of Malondialdehyde (MDA). A brief overview. Chromatographia, 75(10): 433 - 440.
28. Mahmoud, H. H. (2016). New Method for Assessment of Serum Catalase Activity. Indian Journal of Science and Technology. Vol 9 (4)
29. Thulfegar, A., & Mahoud H. (2020). New Spectrophotometric Method for the Assessment of Catalase Enzyme Activity in Biological Tissues. *Current Analytical Chemistry.* Vol 16 98), 2020
30. Mariona, J., Natalia. M. M., Irene. P., Meritxell M.G., Victoria. A., & Reinold.P., (2020). The Advanced Lipoxidation End – Product Malondialdehyde – Lysine in Aging and Longevity. *Antioxidant:* 91132; doi 1033/antiox91132.
31. Pamplona, R. (2008). Membrane Phospholipid Lipoxidative Damage and Molecular Integrity. A casual Role in Aging and Longevity. *Biochemistry* and *Biophysiology,* 1777: 1249 – 1262.
32. Li, F., Yang, Z., Lu, Y., Wei, Y., Wang, J. & Yin, D. (2010). Malondialdehyde suppresses cerebral function by breaking homeostasis between excitation and inhibition in turtle *Trachemys scripta*. *Public Library of Science,* 5(12): 15325 - 15328.
33. Inal, M. E., Kanbak, G. & Sunal E. (2001). Antioxidant enzyme activities and malondialdehyde levels related to aging. *Clinical Chemistry*, 305(1):75 - 80.
34. Kingsley A Okon, Gabriel D Edem, Nsikan-Abasi B Udoh, & Sarah N Umanah (2022) *Rauvolfia vomitoria* remediates neurodegenerative deficiencies in hippocampus of wistar rats treated with lead nitrate. Journal of Advanced Education and Sciences 2022; 2(1):19-23 ISSN NO: 2583-2360 Page | 19
35. Shi. Z., Zhang, Y., Meek, J., Qiao, J., & Han, V.Z. (2008). The Neuronal Organization of a Unique Cerebellar Specialization: The Valvula Cerebelli of a Mormyrid Fish. Neurology. 509 (5): 449–473

36. Pagnussat, A. S., Faccioni-Heuser, M. C., Netto, C. A. & Achaval, M. (2007). An Ultrastructural Study of Cell Death in the CA1 Pyramidal Field of the Hippocapmus in Rats Submitted to Transient Global Ischemia Followed by Reperfusion. *Journal of Anatomy*, 211 (5): 589 – 599
37. Ubong P. Jonah, Nsikan-Abasi B. Udoh, and Lydia E. Udofia (2022) Studies on the Use of Root Extracts of *Triclisia subcordata* and *Hippocratea africana* on the Neurohistology of the Cerebellum of Adult Wistar Rats. *Asian Journal of Research and Reports in Neurology 5(2): 27-36, 2022; Article no. AJORRIN.89227* https://www.sdiarticle5.com/reviewhistory/89227
38. Moses Bassey Ekong, Ubong Udo Ekpene, Fyneway Enang Thompson, Aniekan Imo Peter, Nsikan-Abasi Bassey Udoh, Gabriel Joseph Ekandem (2014) Effects of co-treatment of *Rauwolfia vomitoria* and *Gongronema latifolium* on neurobehaviour and the neurohistology of the cerebral cortex in mice Internet Journal of Medical Update.2015January;10(1):310. doi:10.4314/ijmu. v10i1.2 http://www.akspublication.com/ijmu
39. Ravi, J., Michelle, L,, Sheng-Han, K., Jean-Paul, G., Vonsattel, M. D., & Elan, D., Louis (2014) Cellular Density in the Cerebellar Molecular Layer in Essential Tremor, Spinocerebellar Ataxia, and Controls. *Parkinsonism,* 20 (11): 1270–1273.
40. Ekrem, M., Ignacio, R., Ingeborg, H., Alessandro, G., Bashkim, K., Qiaoyan, H., John, M. & Erminio, C. (2010). Lower Number of Cerebellar Purkinje neurons In Psychosis is Associated with Reduced Reelin Expression. *PNAS,* 107 (9): 4407–4411
41. Ferrer I. g., Santpere G.W., & F.W. Van Leeuwen (2008): Argyrophilic grain Disease. *Brain,* 131;1416-1432.
42. Mitra, N. K., Nadarajah, V. D. & Siong, H. H. (2009). Effect of concurrent application of heat, swim stress and repeated dermal application of chlorpyrifos on the hippocampal neurons in mice. *Folia Neuropathologica*, 47(1): 60 - 68.
43. Pekny, M. & Nilsson, M. (2005). Astrocyte Activation and Reactive Gliosis. *Glia* 50 (8): 427–434.
44. Verkhratsky, A. N & Arthur Butt. (2007). Glial Neurobiology. *Neuroglia,* WL, 102 V519g, 2007
45. Tani, A. S., Allen, N J., Barres, B. A. (2005). Signaling between glia and neurons: focus on synaptic plasticity. *Current Opinion* 9 (2): 37-49.